Observation of swell dissipation across oceans

Fabrice Ardhuin, Bertrand Chapron, Fabrice Collard

Auxiliary material for "Strong decay of steep swells observed across oceans"

Fabrice Ardhuin[1*], Fabrice Collard[3], and Bertrand Chapron[2],

[1]Service Hydrographique et Ocanographique de la Marine, 29609 Brest, France
[2]Laboratoire d'Océanographie Spatiale, Ifremer,
Centre de Brest, 29280 Plouzané, France
[3]BOOST-Technologies, 29280 Plouzané, France

[*]To whom correspondence should be addressed; E-mail: ardhuin@shom.fr.

Swell track combination and SAR data selection

After applying our data selection criteria, only 22 swell track ensembles gave reliable estimates of the swell attenuation. Tables 1 and 2 gives information on these 22 track ensembles only. The original swell partition parameters along these and other swell tracks are available at `http://tinyurl.com/7q7jps`.

Estimation of dissipation coefficients

For each set of SAR data, a function $\widehat{H}_{ss}(\alpha)$ was fitted. Three fits were performed, one with a constant linear decay μ, the others with constant dissipation factors $f_{e,s}$ or f_e. In each case the parameter α, f_e or $f_{e,s}$ was fitted together with the height $H_{ss}(\alpha_0)$ at a distance $x_0 = R\alpha_0 = 4000$ km from the storm source.

In practice, we scanned the possible values of $H_{ss}(\alpha_0)$, from 1 to 12 m, and μ or $f_e/f_{e,s}$ (from -2.0×10^{-7} to 1×10^{-6} m^{-1} and -0.1 to 0.4, respectively), and the pair ($\widehat{H}_{ss}(\alpha_0)$,$\mu$), ($\widehat{H}'_{ss}(\alpha_0)$, $f_{e,s}$), or ($\widehat{H}''_{ss}(\alpha_0)$, f_e) that gave the minimum root mean square difference with observations $H_{ss}(\alpha_i)$ was retained (table 2).

In order to perform this fit, the function $\widehat{H}_{ss}(\alpha)$, was obtained from a numerical integration of

$$\frac{\mathrm{d}\left(E_s \alpha \sin\alpha\right)}{\mathrm{d}\alpha} = \mu R E_s \alpha \sin\alpha \tag{1}$$

number	Storm time	Latitude	Longitude	T	$\theta_{\min}$	$\theta_{\max}$	N
1	20040216 0000	160 E	37 N	14	76	85	32
2	20040216 0000	160 E	37 N	15	85	95	21
3	20040418 1800	165 W	52 S	14	63	94	9
4	20040418 1800	165 W	52 S	15	85	90	14
5	20040418 1800	165 W	52 S	16	77	88	26
6	20040418 1800	165 W	52 S	17	75	85	26
7	20040630 2359	145 E	25 N	13	75	80	23
8	20040709 1800	177 E	55 S	14	32	37	10
9	20051021 0000	155 W	50 N	15	120	130	11
10	20051113 1208	160 E	40 N	15	85	95	40
11	20051113 1208	160 E	40 N	17	80	90	24
12	20060310 0000	137 W	45 N	16	140	150	16
13	20060310 1200	136 W	45 N	14	145	155	10
14	20060310 2300	136 W	45 N	13	130	140	8
15	20060427 0000	155 W	54 S	15	65	75	37
16	20060427 0600	150 W	58 S	14	65	75	34
17	20060427 0600	143 W	53 S	16	35	45	16
18	20070212 1800	168 E	38 N	15	74	90	35
19	20070812 0000	100 W	55 S	15	-30	-24	19
20	20070812 0000	100 W	55 S	17	-27	-17	14
21	20070812 0000	100 W	55 S	18	-27	-17	8
22	20071030 0000	155 W	47 S	15	75	90	45
Units	date and hour UTC	deg.	deg.	s	deg.	deg.	

Table 1: Ensembles of swell tracks selected for swell attenuation analysis. Each ensemble is defined by the source storm, the minimum and maximum outgoing directions $\theta_{\min}$ and $\theta_{\max}$. The number of SAR data that was retained for the estimation of the attenuation is N. All storms are located in the Pacific Ocean.

or

$$\begin{aligned} \frac{\mathrm{d}\left(E_s \alpha \sin\alpha\right)}{\mathrm{d}\alpha} &= 16\frac{\rho_a}{\rho_w}\left(f_{\mathrm{e,s}} \quad \text{or} \quad \gamma f_{\mathrm{e}}\right)\frac{32\pi^4}{gT^4} R E_s^{1.5} \alpha \sin\alpha \\ &\qquad \text{if} \quad \mathrm{Re_s} > 28000 \quad \text{or} \quad \mathrm{Re} > 100000 \\ \frac{\mathrm{d}\left(E_s \alpha \sin\alpha\right)}{\mathrm{d}\alpha} &= \mu_v R E_s \alpha \sin\alpha \quad \text{otherwise,} \end{aligned} \tag{2}$$

where γ is $\max\{1.5, u_{\mathrm{orb}}/u_{\mathrm{orb,s}}\}$, in which the minimum value of 1.5 is meant to correct for the systematic underestimation of u_{orb} by the numerical model for the large swells wave heights.

Numerical integrations were performed from $x = 4000$ to $x = 15000$ km, for each pair, e.g. $(\widehat{H}_{ss}(\alpha_0), \mu)$, using a simple first order Euler scheme that was found to converge fast enough.

number	μ	μ_1	μ_2	H	ε_1	Re_s	$f_{e,s}$	f_e	ε_2	U_{10}
1	26.0	22.3	29.3	5.7	7	10.4	0.0144	0.0119	12	6.0
2	20.3	16.1	25.9	4.0	16	4.8	0.0149	0.0114	16	5.8
3	20.8	3.6	36.6	3.4	14	3.7	0.0113	0.0075	14	5.5
4	5.1	-8.0	16.8	2.6	8	2.0	0.0069	0.0046	8	5.6
5	11.7	5.3	18.3	2.9	10	2.4	0.0083	0.0055	10	7.1
6	8.6	2.7	15.1	2.8	10	2.1	0.0053	0.0035	10	6.9
7	9.9	2.5	18.6	2.1	23	1.5	0.0053	0.0036	23	5.1
8	10.3	-6.5	24.4	2.2	8	1.6	0.0042	0.0028	8	5.4
9	11.7	7.5	15.1	3.4	9	3.5	0.0142	0.0130	13	6.4
10	9.2	4.8	13.8	2.5	16	1.9	0.0198	0.0131	16	5.8
11	6.0	-5.8	6.2	2.4	11	1.5	-0.0002	-0.0003	11	6.2
12	4.4	0.0	9.6	2.4	9	1.6	0.0041	0.0028	9	6.2
13	10.1	4.1	16.2	2.0	7	1.3	0.0111	0.0054	7	6.5
14	9.2	-1.4	19.3	2.1	9	1.5	0.0208	0.0074	11	6.7
15	9.6	5.8	13.3	3.6	8	3.9	0.0051	0.0034	8	6.1
16	15.9	9.2	22.2	3.3	6	3.5	0.0043	0.0029	6	6.7
17	8.8	-1.2	18.5	3.0	6	2.5	0.0074	0.0049	5	5.7
18	35.9	31.5	40.2	4.4	8	5.8	0.0259	0.0190	8	6.2
19	-2.2	-6.7	2.4	1.6	12	0.8	-0.0039	-0.0039	11	6.0
20	-2.3	-9.7	3.5	1.4	11	0.5	-0.0064	-0.0032	11	6.8
21	-5.5	-13.0	3.0	1.1	17	0.3	-0.0081	-0.0081	17	7.3
22	19.7	13.4	25.9	2.7	13	2.2	0.0200	0.0110	12	6.5
Units	10^{-8} m^{-1}	10^{-8} m^{-1}	10^{-8} m^{-1}	m	%	10^5			%	m s^{-1}

Table 2: Swell dissipation estimates. The fitted wave height at 4000 km from the source and constant linear decay coefficients are $H = \widehat{H}_{ss}(\alpha_0)$ and μ, with ε_1 the mismatch of the linear attenuation to the observed wave heights, normalized by the r.m.s. observed height. The analysis was repeated 400 times using a Monte Carlo simulation of observation errors. The 16% and 84% levels in the estimation of μ are given by μ_1 and μ_2. The fitted swell dissipation factor and total dissipation factor are $f_{e,s}$ and f_e, the latter with a relative error ε_2. Finally the mean wind speed over the SAR images used in the fit is also given by U_{10}, and the significant swell Reynolds number Re_s is estimated at 4000 km from T and H obtained from the linear fit, as $\mathrm{Re}_s = 2\pi H^2/(\nu T)$.

Here the swell Reynolds number is defined as $\mathrm{Re}_s = 4u_{\mathrm{orb},s}a_{\mathrm{orb},s}/\nu$. The wind sea and other swell systems are taken into account in the f_e fits via the γ factor. The error function was computed by linearly interpolating the discretized $H'_s(\alpha_j)$ at the positions α_i where selected observations were made.

In order to take into account the uncertainty of the SAR-derived wave heights, the estimation of μ was repeated 400 times using uncorrelated random values of each SAR measurement, using the error model (section 2 of the paper). This Monte-Carlo estimation gave 400 values of μ and H. The values corresponding to the 16 and 84 percentiles (this would correspond to one standard deviation if the values were Gaussian), are given in table 2 and shown as error bars on figure 1 of the paper.

The estimated swell dissipation coefficient μ was found to be weakly sensitive to the exact choice of the distance x_0 and the minimum and maximum values for the wind speed and wave height. The variability of values of μ for any range of wave slope is limited, and the confidence intervals of most of the estimates are relatively narrow. This suggests that our analysis is more accurate than previous studies, in which attenuations less than 1.0×10^{-7} m^{-1} were not reliable (this value corresponds to 0.05 dB/degree in Snodgrass et al. 1966). This was likely due to the misalignement of swell tracks with fixed measuring stations, and errors introduced by corrections for islands, problems that are absent in our dataset.

On the contrary, the estimation of f_e is limited by the known biasses of the model described by Ardhuin et al. (2009), used here to estimate the significant surface orbital velocity amplitude u_{orb}. Indeed, $u_{\mathrm{orb}} = 2\pi H_s/T_{m02}$, and although both H_s and T_{m02} are accurately estimated for average sea states, up to $H_s = 8$ m, there is a strong negative bias on wave heights in big storms, (for $H_s > 10$ m the bias is of the order of 10 to 15% of the observed value), which is typical of conditions found in some cases here. We have thus corrected u_{orb} values from the model to be at least 1.5 times the SAR-derived swell orbital velocity $u_{\mathrm{orb,s}}$. The values of f_e are thus indicative, and are not expected to have a relative accuracy better than 50%.

Discussion. Boundary layer theory without wind

For the sake of simplicity we will consider here the case of monochromatic waves propagating in the x direction only, and we will neglect the curvature of the surface. For the small steepness swells considered here that latter approximation is well founded and a more complete analysis is given by Kudryavtsev et Makin (2004). The free stream velocity above the waves, just outside of the boundary layer is $u_+(x,t) = -\sigma a \cos(kx - \sigma t)$, where a is the swell amplitude and $\sigma = 2\pi/T$ is the radian frequency. The sub-surface velocity is $u_-(x,t) = \sigma a \cos(kx - \sigma t)$ (figure 1). Due to the oscillations that propagate at the phase velocity C, the horizontal advection of any quantity X by the flow velocity u, given by $u\partial X/\partial x$, can be neglected compared to its rate of change in time $\partial X/\partial t$ since the former is a factor u/C smaller than the latter, which is typically less that 0.1 for the swells considered here. Defining $\widetilde{u}(x,z,t) = \langle u(x,z,t)\rangle - u_-(x,t)$, where the brackets denote an average over flow realizations for a given wave phase. The horizontal

momentum equation is thus approximated by,

$$\frac{\partial \widetilde{u}}{\partial t} = -\frac{1}{\rho_a}\frac{\partial p}{\partial x} - \frac{\partial u_-}{\partial t} + G \tag{3}$$

where G represents the divergence of the vertical viscous and turbulent fluxes of horizontal momentum,

$$G = \nu \frac{\partial^2 \widetilde{u}}{\partial z^2} + \frac{\partial \left\langle u'w' \right\rangle}{\partial z}. \tag{4}$$

Because the boundary layer thickness δ is small compared to the wavelength, the pressure gradient in the boundary layer is given by the pressure gradient above the boundary layer, in balance with the horizontal acceleration. This is another way to write Bernoulli's equation (e.g. Mei 1989),

$$-\partial p/\partial x/\rho_a = -\sigma^2 a \sin(kx - \sigma t) = \partial u_+/\partial t. \tag{5}$$

This yields

$$\frac{\partial \widetilde{u}}{\partial t} = 2\frac{\partial u_+}{\partial t} + G \tag{6}$$

with the boundary condition for $z \gg \delta$, $\widetilde{u}$ goes to $2u_+(x,t)$. The equation for the horizontal momentum is thus exactly identical to the one for the oscillatory boundary layer over a fixed bottom with wave of the same period but with an amplitude twice as large. In the viscous case, one recovers, after some straightforward algebra, the known viscous result, i.e., for $z > \zeta$,

$$\widetilde{u}(x,z,t) = 2\sigma a \left[\mathrm{e}^{z_+} \cos\left(kx - \sigma t + z_+\right) - \cos\left(kx - \sigma t\right)\right] + O(\rho_a/\rho_w) \tag{7}$$

where $z_+ = (z-\zeta)/\sqrt{2\nu/\sigma}$, with the surface elevation $\zeta(x,t) = a\cos(kx - \sigma t)$. Evaluating the work of the viscous stresses $\langle \rho_a \nu u \partial u/\partial z \rangle$, eq. (7) gives the low frequency asymptote to the viscous decay coefficient, $\mu_v = 2k\sqrt{2\nu\sigma}\rho_a/\rho_w/C_g$. This result was previously obtained using a Lagrangian approach without all the above simplifying assumptions (Weber and Forland 1990). The full viscous result is obtained by also considering the water viscosity ν_w, which gives the $O(\rho_a/\rho_w)$ correction for the motion in the air, and the classical dissipation term with a decay $\mu_{vw} = 4k^2\nu_w/C_g$, which dominates for the short gravity waves.

As a result, for a comparison with fixed bottom boundary layers, the Reynolds number based on the orbital motion should be redefined with a doubled velocity and a doubled displacement, i.e. Re$= 4u_{\mathrm{orb}}a_{\mathrm{orb}}/\nu$. For monochromatic waves $a_{\mathrm{orb}} = a$ and $u_{\mathrm{orb}} = a\sigma = 2\pi a/T$. For random waves, investigations of the ocean bottom boundary layer suggest that the boundary layer properties are roughly equivalent to that of a monochromatic boundary layer defined by significant properties (Traykovski et al. 1999).

Although the wind was neglected here, it should influence the shear stresses when its vertical shear is of the order of the wave-induced shear. Taking a boundary layer thickness δ and wind friction velocity $u_\star$, and assuming a logarithmic wind profile, this should occur when $u_\star/(\kappa\delta)$ exceeds $2u_{\mathrm{orb}}/\delta$, where κ is von Kármán's constant. This corresponds to, roughly, $u_\star > u_{\mathrm{orb}}$. For swells with T < 15 s and $H_{ss} > 2$ m (i.e. $u_{\mathrm{orb,s}} > 0.4$ m s^{-1}), and winds less than 7 m s^{-1}

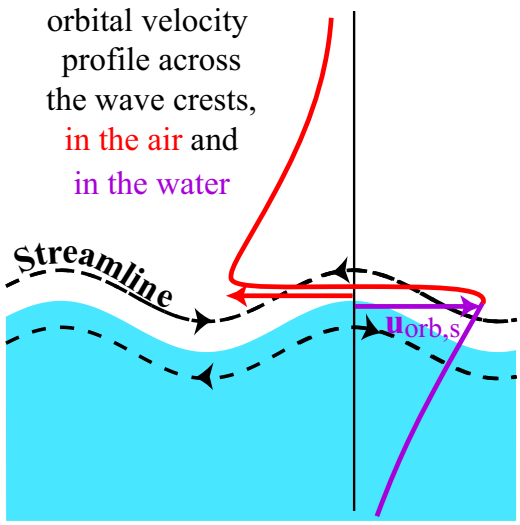

Figure 1: Boundary layer over waves in the absence of wind. Because of the larger inertia of the water compared to the air, most of the adjustment from the sub-surface velocity to the free stream velocity in the air occurs on the air-side of the surface.

(i.e. $u_\star < 0.2$ m s^{-1}), the wind effect on f_e may be small and the previous analysis is likely valid. In general, however, the nonlinear interaction of the wave motion and wind should be considered, which requires an extension of existing theories for the distortion of the airflow to finite swell amplitudes.

References

[*Ardhuin et al.*(2008)*Ardhuin, Collard, Chapron, Queffeulou, Filipot, and Hamon*] Ardhuin, F., F. Collard, B. Chapron, P. Queffeulou, J.-F. Filipot, and M. Hamon (2008), Spectral wave dissipation based on observations: a global validation, in *Proceedings of Chinese-German Joint Symposium on Hydraulics and Ocean Engineering, Darmstadt, Germany*.

[*Ardhuin et al.*(2009)*Ardhuin, Marié, Rascle, Forget, and Roland*] Ardhuin, F., L. Marié, N. Rascle, P. Forget, and A. Roland (2009), Observation and estimation of Lagrangian, Stokes and Eulerian currents induced by wind and waves at the sea surface, *J. Phys. Oceanogr.*, submitted, available at http://hal.archives-ouvertes.fr/hal-00331675/fr/.

[*Kudryavtsev and Makin*(2004)] Kudryavtsev, V. N., and V. K. Makin (2004), Impact of swell on the marine atmospheric boundary layer, *J. Phys. Oceanogr.*, *34*, 934–949.

[*Mei*(1989)] Mei, C. C. (1989), *Applied dynamics of ocean surface waves*, second ed., World Scientific, Singapore, 740 p.

[*Snodgrass et al.*(1966)*Snodgrass, Groves, Hasselmann, Miller, Munk, and Powers*] Snodgrass, F. E., G. W. Groves, K. Hasselmann, G. R. Miller, W. H. Munk, and W. H. Powers (1966), Propagation of ocean swell across the Pacific, *Phil. Trans. Roy. Soc. London, A249*, 431–497.

[*Traykovski et al.*(1999)*Traykovski, Hay, Irish, and Lynch*] Traykovski, P., A. E. Hay, J. D. Irish, and J. F. Lynch (1999), Geometry, migration, and evolution of wave orbital ripples at LEO-15, *J. Geophys. Res.*, *104*(C1), 1,505–1,524.

[*Weber and Førland*(1990)] Weber, J. E., and E. Førland (1990), Effect of the air on the drift velocity of water waves, *J. Fluid Mech.*, *218*, 619–640.